Surface modification of spring tine cultivator points with different metal powders by GTAW method

K. Can[1] and I.S. Dalmis[1,*]

[1]*Mechanical Engng. Department, Tekirdağ Namık Kemal University, 59860 Corlu Tekirdag, Turkey.*
***Corresponding author**: idalmis@nku.edu.tr

ABSTRACT The abrasive wear resistance of soil tillage tools is important for the agricultural equipment industry because abrasive wear caused by hard particles in the soil can shorten the lifespan of these parts. In this study, surface modification using FeCrC, FeTi, and Ni powders was carried out to improve the hardness and wear resistance of AISI 1040 material reversible spring tine cultivator points. The GTAW (Gas Tungsten Arc Welding) method was chosen for the energy input in the surface modification process due to its simplicity and efficiency. Microstructure studies were conducted using an optical microscope (OM), scanning electron microscope (SEM), energy-dispersive X-ray spectroscopy (EDS), and X-ray diffraction (XRD). Additionally, microhardness measurements and wear tests were performed. It was found that the hardness values for all three coating types were higher than the ones measured in the substrate material. The maximum microhardness was 726.1 HV0.2 for the coating with a 70FeCrC + 30FeTi composition ratio. As a result of the increased hardness in the coating layer of the specimens, the wear resistance also increased. Abrasive wear tests were conducted under loads of 5 N, 10 N, and 15 N at distances of 400 m, 800 m, and 1200 m, respectively. The weight loss of the substrate was about 13 times higher compared to the coating containing 70FeCrC + 30FeTi. After the laboratory tests, cultivator points were coated and field tests were carried out.

KEYWORDS Abrasive wear; Cultivator points; GTAW; Surface modification; Tillage tools

1. Introduction

The general problem experienced in tillage tools used in the agricultural industry is the wear of the points. Material engineers and researchers have experimented with different methods to increase the wear resistance of agricultural equipment points. In recent years, surface coating technologies have been widely preferred (Singh et al., 2021; Singh and Singh Chatha, 2020; Kostencki et al., 2019).

Wear is a continuous loss of material that occurs on a surface (Sabet et al., 2011; Cheng et al., 2008). There are different types of wear cases according to the basic material loss and wear mechanisms. According to their wear mechanisms, they can be divided into adhesive wear, abrasive wear, fatigue wear and wear caused by tribochemical reactions. In addition, one or more wear mechanisms may occur on the contact surfaces at the same time (Axen et al., 2001). For years, machinery manufacturing products have been widely used in numerous fields such as building, mining and emergency rescue. However, parts operating in harsh operating conditions can be damaged quickly due to wear in a short time (Chen et al., 2018). Zabala et al. (2019) evaluated the influence of surface roughness in steel on wear using a pin-on-disc test. They concluded that abrasion of the fixed components was decreased when the roughness of the moving surface was increased. Wear affects the life of the parts, their dimensions and consequently the quality of the parts produced. Wear is of high importance in many parts and components that need to be constantly replaced and repaired (Burwell, 1957).

Abrasive wear is one of the most common mechanisms for material losses caused by wear in the industry (Binder et al., 2017; Blau and Dehoff, 2013; Eyre, 1976) and it constitutes one of the main problems of tillage machines in the agricultural sector (Kang et al., 2017; Bayhan, 2006; Kang et al., 2014; Singh et al., 2021; Sundström et al., 2001; Zdravecká et al., 2014). Wear in the agricultural industry causes loss of time, labor and energy as well as equipment replacement costs (Kang et al., 2017; Kalácska et al., 2020). In addition, tools working under the ground are also exposed to high-impact loads due to the stones in the soil. For this reason, the materials of these tools must be resistant to both abrasion and impact loads (Kang et al., 2017).

Cultivators are widely used in tillage. The reason for this is that they are not complicated, quite simple to use, and cost-effective (Polat et al., 2012; Gokcebay, 1998). Cultivator points have high importance among tillage tools. Since they are exposed to intensive abrasion in the soil, they are required to have high abrasion resistance (Gulec and Altuntaș, 2013).

A technique known as specifically targeted surface modification has been proposed by researchers to improve the surface properties of materials (Nair et al., 2018). The coating process provides superior properties such as strength, hardness, and resistance to abrasion and corrosion in materials. It can be separated according to the purpose of the coating, the type of material, the thickness of the coating, the cost of the applied method and the ease of application (Orhan, 2008). Many researchers have used traditional coating techniques such as physical vapor plating, chemical vapor plating, spray plating, chrome plating, etc. In addition, the surface is modified by using a laser, electron beam and GTAW method as the heat source.

DOI: 10.52292/j.laar.2024.1063
Received: May 11, 2022.
Accepted: April 4, 2023.
Recommended by Germán Prieto.

The benefit of these methods is the formation of a whole piece with the substrate after solidification compared to traditional methods (Nair et al., 2018).

Researchers have conducted studies on improving the wear resistance of tillage tools. Some of the methods used in these studies are manual metal arc welding (MMAW) (Singh et al., 2021; Singh and Singh Chatha, 2020; Kang et al., 2017), laser cladding method (Bartkowski and Bartkowska, 2017), thermal spray coating (Kang et al., 2012) and arc PVD method (Malvajerdi et al., 2019).

Recently, the use of the surface modification technique with the GTAW method has been the subject of interest by many researchers (Yilmaz, 2006; Iwaszko, 2006; Liu et al., 2008; Erdogan et al., 2010; Kumar et al., 2017; Ardeshiri et al., 2017; Ya-long et al., 2018; Mithun et al., 2018). Tungsten Inert Gas (TIG) or Gas Tungsten Arc Welding (GTAW) method is a process where hard surface coatings can be made with low heat input because of the economical and easy adjustment of welding parameters (Yilmaz, 2009). The fact that the GTAW method is cheaper than laser and electron beam makes it stand out (Ardeshiri et al., 2017). In the surface modification using the GTAW method, the penetration of the powders adhered to the substrate material is ensured by the energy transferred to the welding area with the non-melting tungsten electrode (Islak and Yildirim, 2009). Until now, many powders have been used as coating powder in the surface coating process such as WC, Cr_3C_2, $MoSi_2$, WC, Co, Fe, Si, NiCrBSi, Ti, and FeCrC for the coating process (Yilmaz, 2006; Liu et al., 2008; Erdogan et al., 2010; Ardeshiri et al., 2017; Ya-long et al., 2018; Mithun et al., 2018; Ghadami et al., 2015).

In this study, the coating ability of the surface of the s-tine cultivator point, which is one of the most used tools in the agricultural industry (Gulec and Altuntaş, 2013), was investigated by the GTAW method to improve the wear properties. FeCrC, FeTi and Ni powders were used as coating powder in the experiments. The substrate is AISI 1040 steel. Studies were carried out both in field and laboratory conditions. Microstructure images were examined under laboratory conditions. In addition, microhardness and wear tests were carried out. In the field tests, in addition to carrying out the abrasion tests according to the weight-loss method, the changes in the cultivator point dimensions based on their profiles were examined with the 3D scanning processes.

2. Methods

The research was carried out in two stages: laboratory tests and field tests. The purpose of the laboratory tests was to determine the abrasion performance of the powders before the field tests, in order to ensure that the field experiments could be more accurately interpreted. Middle-carbon steel AISI 1040, a material commonly used in cultivator points, was used as the substrate in the laboratory tests. The chemical compositions of the powders and the substrate are shown in Table 1. The specimens were cleaned with sandpaper and acetone to remove dirt and rust from their surfaces. A small amount of sodium silicate was used to fix the powders in the 8 mm channels with a 1 mm depth that were opened on the 10 mm part of the specimens (Fig. 1). The specimens were then dried in an oven at 100 °C for 30 minutes to remove moisture. The powders were prepared from a mixture of FeCrC, FeTi, and Ni powders and applied to the material surface using the water-cooled 'Lincoln Invertec® V205-T AC/DC' TIG welding machine as an external energy input. To avoid using a thorium electrode, which is radioactive, a 1.5 % lanthanum alloy tungsten electrode was used instead. The coating process parameters are given in Table 2. The GTAW process (Can et al., 2022) was used in the welding setup to ensure the continuity of the surface coating processes.

The coating powder mixture ratios of the specimens are given in Table 3.

The mechanism used was PLC-controlled, allowing for easy control of parameters such as welding speed and torch height, which are difficult to adjust manually. The specimens were ground using 320, 480, 600, 800, and 1000 mesh SiC sandpaper and then polished with 3-micrometer diamond paste. The polished specimens were washed with water and dried. To obtain images using an optical microscope, the specimens were etched with a solution of 5 mL $FeCl_3$, 15 mL HCl, and 50 mL distilled water for 30-45 seconds. The specimens were then dried with hot air and the standard metallographic specimen preparation processes were completed. The microstructure and chemical composition of the cladding layer were observed using optical microscopy and scanning electron microscopy (SEM). The crystal structures of the cladding layer were identified using X-ray diffraction analysis. Hardness values were taken from the upper surface of the coating area at 0.5 mm intervals under a 200 gf load, with a 10-second wait time. The abrasive wear test was conducted on a device designed according to ASTM G174-04 standard using 80 mesh SiC sandpaper as the abrasive. A new piece of sandpaper was used for each wear test. The tests were conducted over wear distances of 400 m, 800 m, and 1200 m under loads of 5 N, 10 N, and 15 N. To shorten the duration of the tests, the speed was kept high and the time-dependent path was calculated as 400 m per minute based on the motor speed. After the laboratory tests, surface modification was performed on the

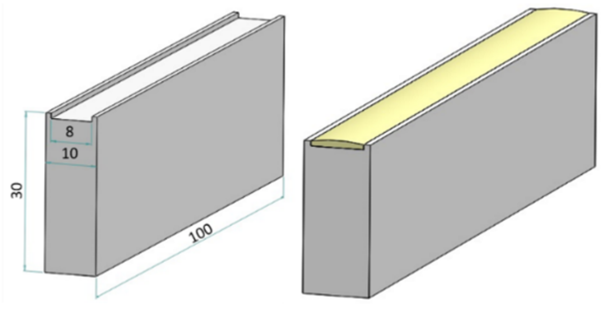

Figure 1: Dimensions and schematic view of specimens with powder adhered to its surface used in coatings for laboratory test.

Table 1: Chemical compositions of substrate and powders (wt. %).

Material	C	Mn	P	S	Si	Cr	Ti	Al	Ni	Fe
Substrate	0.4	0.6	0.04	0.05	0.25	-	-	-	-	Balance
FeCrC	6.2	-	0.03	0.02	1.5	64	-	-	-	Balance
FeTi	0.11	-	-	0.008	0.05	-	70.35	3.86	-	Balance
Ni	-	-	-	-	-	-	-	-	99.99	Balance

Table 2: Coating process parameters.

Process parameters	Unit	Value
Electrode diameter	mm	2.4
Current	A	160
Voltage	V	16.4
Welding speed	mm/min	100
Shielding gas flow rate	L/min	14
Distance between electrode and workpiece	mm	2
Electrode tip angle	Degree	180

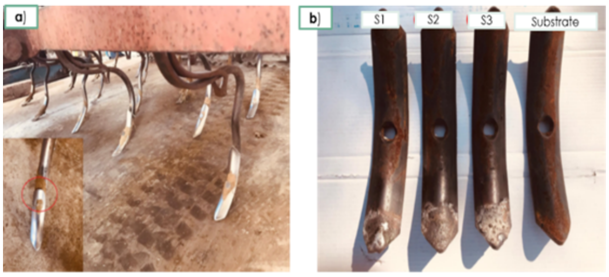

Figure 3: Cultivator points, a) Worn points, b) Coated points by GTAW.

Table 3: Coating powder mixture ratios of the specimens (wt. %)

Specimen	FeCrC	FeTi	Ni
S1	100	-	-
S2	70	30	-
S3	64	16	20

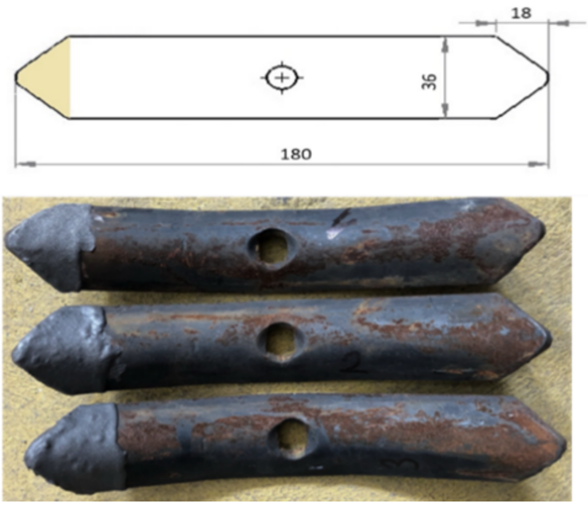

Figure 2: Dimensions of cultivator points.

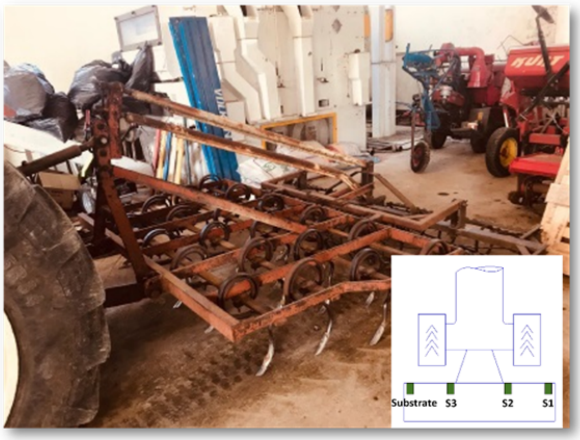

Figure 4: Spring cultivator used in studies and location of points.

cultivator points, specifically on the tips where wear typically begins. All the procedures applied to the specimens prepared for the laboratory tests were also applied manually to the cultivator points. 3.5 g of powder was used in the coatings, which were applied to an area of approximately 300 mm^2 by mixing the powders homogeneously with sodium silicate (Fig. 2). In the preliminary field tests, it was observed that the cultivator points were wearing from their tips. Farmers typically reverse the worn points and use the other sides (Fig. 3a). Figure 3b shows cultivator points coated with GTAW. Field tests were carried out for 3.5 hours on an area of 60 decares with a clay-loam soil structure on the campus of Tekirdag Namik Kemal University. The latitude and longitude coordinates of the test field are 40.997452 and 27.592737, respectively. Soil compaction was measured using a hand-pushed electronic cone penetrometer (Eijkelkamp Penetrologger 06.15.SA) and was found to be in the range of 1.5-2 MPa. In the field experiments, an Aysan AYK-21 model spring cultivator with 21 feet was used. The placement of the cultivator points is shown in Fig. 4. In order to observe the wear behavior of the cultivator points, their weight was measured before and after the field tests, and 3D scanning was carried out using the GOM Atos Compact model optical scanner.

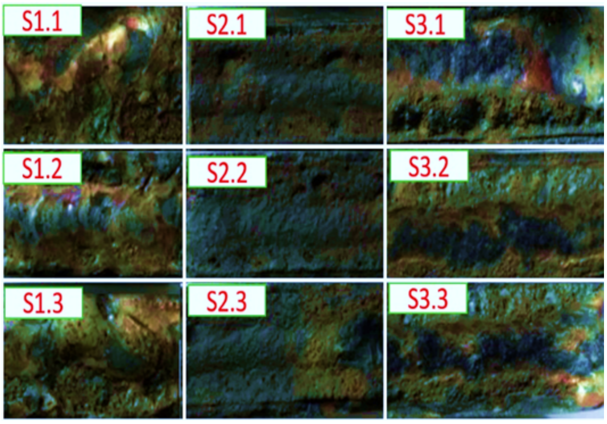

Figure 5: Images of coated specimens.

3. Results

Figure 5 shows images of the coated surfaces of the specimens. It can be seen that the melting occurred well, the coating layer had a smooth structure, and there were no defects such as pores or macro cracks.

An optical microscope image of the S1 specimen is shown in Fig. 6a. The high energy input caused significant melting of the substrate material, resulting in dendritic solidification due to the rapid cooling of the structure. (Yilmaz, 2006) stated in his study that solidification in coatings made with FeCrC powders using the GTAW method occurs in a dendritic manner. When the SEM images of the specimen were examined, it was observed that the martensite phase formed in the transition region in a needle-like shape due to the rapid cooling that caused the transformation of the austenite phase into the martensite phase. The martensite phase is a hard and brittle structure, which makes it a potential starting point for cracks and therefore it is not preferred in the welding of carbon steels (Fig. 6b). Figure 6c shows the result of the EDS analysis of the S1 specimen, which demonstrates that solidification occurred as a dendritic structure with a eutectoid structure formed between dendrites. This is considered a hypoeutectoid structure (Dalmis et al., 2018). According to the EDS results, the eutectoid structure (Fig. 6c, Point B) had a higher Cr concentration than the dendritic region (Fig. 6c, Point A). Figure 6d shows the graph of the EDS analysis of the coating layer. The compounds forming the coating layer of the S1 specimen are shown in Fig. 7. M_7C_3 (M = Cr, Fe), α-Fe, and α-M_7C_3 phases were detected in the coating layer.

FeTi was added to FeCrC powders to reduce and orient the grains in the modified region of the S2 specimen. In Fig. 8a, it can be seen that coaxial grains were formed with the effect of the Ti element. The Ti element decreases the activation energy, reduces the surface tension, and increases the nucleation rate during the solidification of metallic materials. Ti significantly reduces grain sizes by increasing the nucleation rate of carbides in the microstructure (Teker et al., 2014). It also provides a homogeneous distribution of carbides in the structure. In this process, with the addition of Ti, the grain size was reduced and a multi-grained structure was formed. Fig. 8b shows the SEM image of the S2 specimen. With the effect of FeTi powders added to FeCrC powders, cubic titanium carbides (TiC) were formed in the grain. In the literature, it has been stated that free titanium forms small cubic TiC particles after the solidification of high carbon melts (Teker et al., 2014). Figure 8c and Fig. 8d show the SEM image of the coating layer of the S2 specimen and the graph of the EDS analysis, respectively. The Ti element's core-forming feature resulted in a fine-grained microstructure. SEM, EDS, and XRD analyses showed that complex carbides formed at the grain boundaries. The compounds forming the coating layer of the S2 specimen are shown in Fig. 9. The XRD analysis results showed the presence of α-M_7C_3, TiC, M_7C_3-TiC, FeCr, α-Fe, FeCr-TiC, and α-TiC phases in the coating layer.

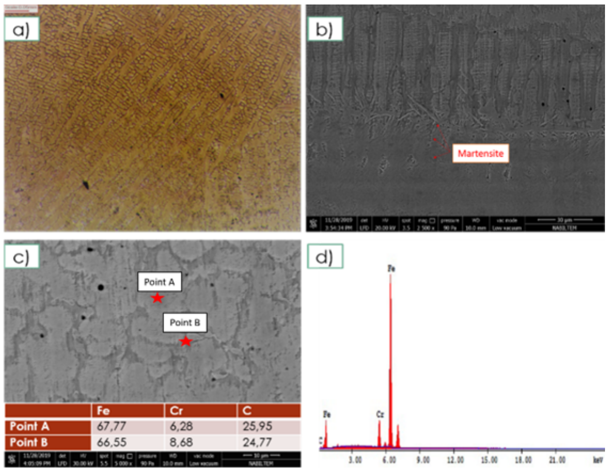

Figure 6: Microstructure of S1 a) Optical image, b) SEM image, c) SEM image and EDS analysis, d) EDS analysis of coating zone.

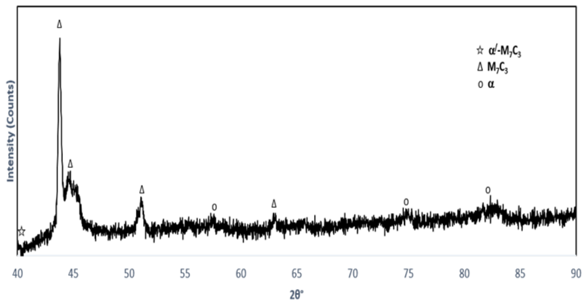

Figure 7: Phase composition of S1.

When the optical microscope image of the S3 specimen was examined (Fig. 10a), a fine-grained dendritic solidification was observed. The addition of Ni decreased the amount of carbide and made the grains smaller. Ni shortened the distance between the secondary dendrite arms (Bal et al., 2019). The distance between the secondary dendrite arms is an important factor in the strength and toughness of the material (Ghassemali et al., 2017). It was determined that the addition of Ni reduced the distance between the secondary dendrite arms by approx-

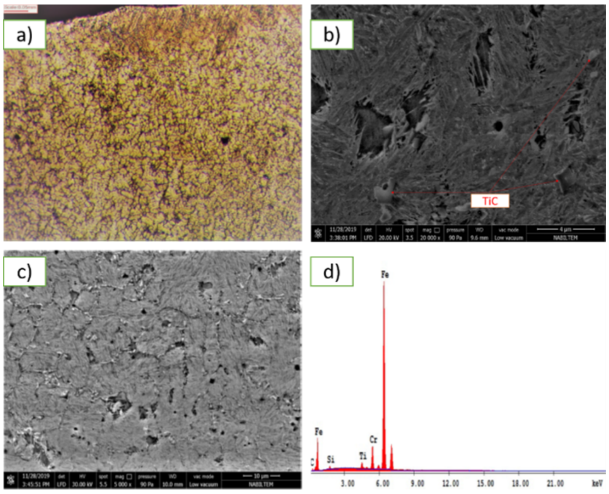

Figure 8: Microstructure of S2 a) Optical image, b) SEM image, c) SEM image and EDS analysis, d) EDS analysis of coating zone.

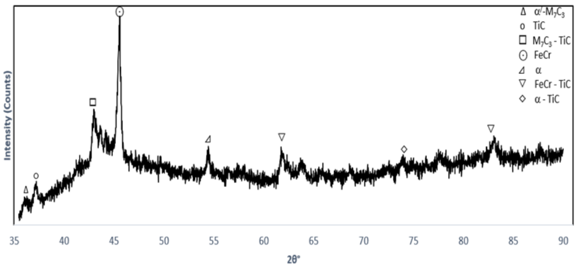

Figure 9: Phase composition of S2.

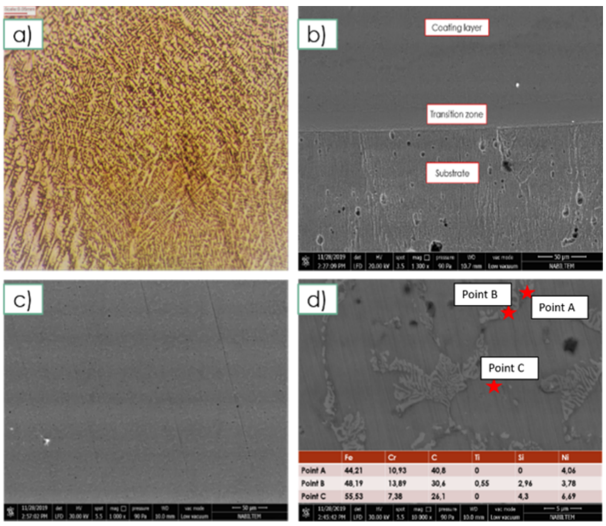

	Fe	Cr	C	Ti	Si	Ni
Point A	44,21	10,93	40,8	0	0	4,06
Point B	48,19	13,89	30,6	0,55	2,96	3,78
Point C	55,53	7,38	26,1	0	4,3	6,69

Figure 10: Microstructure of S3 a) Optical image, b) SEM image of the transition zone, c) SEM image of the coating layer, d) SEM image and points taken EDS analysis.

imately 30-40 %. Theoretically, considering the strong relationship between the distance between the secondary dendrite arms and material strength and hardness, it was thought that the addition of Ni increased the strength and hardness of the modified region on the surface. The den-

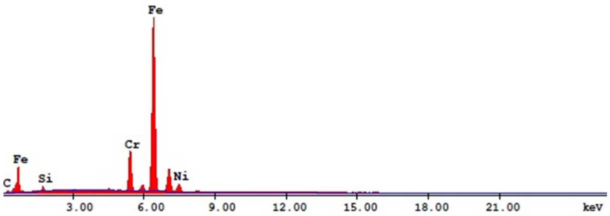

Figure 11: EDS analysis of coating zone for S3 specimen.

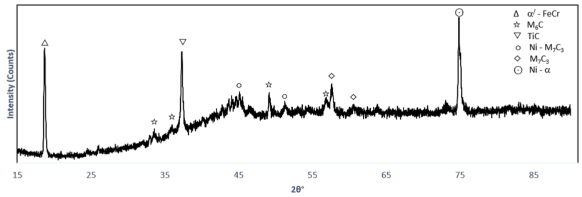

Figure 12: Phase composition of S3.

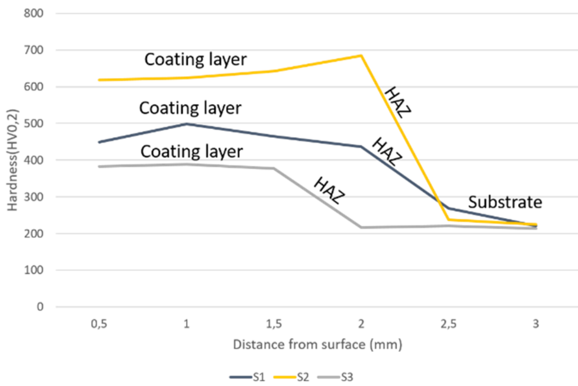

Figure 13: Microhardness results.

drite growth rate and heat capacity are directly proportional, while the melting temperature is inversely proportional. It was thought that the morphology of the dendritic structure changed as the addition of Ni increased the heat capacity of the structure. Figure 10b shows the SEM image of the transition region of the S3 specimen. In addition to FeCrC and FeTi powders, Ni powders were added to the S3 specimen to increase its toughness. The SEM image shows that a narrow transition zone is formed in the specimen, and the coating zone consists of fine-grained dendrites (Fig. 10c and Fig. 10d). EDS and XRD analyses showed that chromium, which was pushed to the grain boundaries due to nickel, formed complex chromium carbides at the grain boundaries. Figure 10d shows the results of the EDS analysis of the region. Figure 11 shows the compounds forming the coating layer of the S3 specimen. The XRD analysis results showed the presence of α-FeCr, M_6C, TiC, Ni-M_7C_3, M_7C_3, and Ni-α phases in the coating layer.

Microhardness values of specimens are given in Figure 13. The average microhardness value in the coating area of S1 specimen was 469.96 $HV_{0,2}$, S2 specimen was 642.29 $HV_{0,2}$ and S3 specimen was 382.9 $HV_{0,2}$. Maxi-

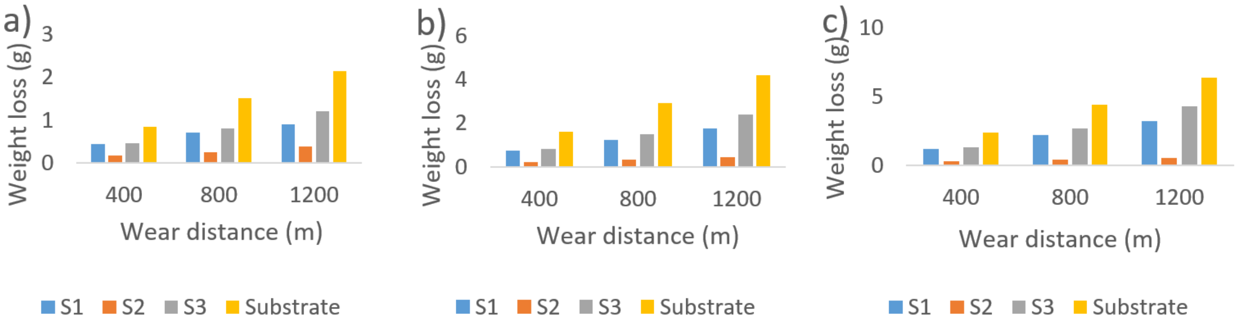

Figure 14: Wear results in laboratory tests, a) 5 N, b) 10 N, c) 15 N.

mum microhardness values for S1, S2 and S3 were 593.4 $HV_{0,2}$, 726.1 $HV_{0,2}$ and 396.1 $HV_{0,2}$, respectively.

According to the results, the addition of FeTi to FeCrC powders caused a significant increase in hardness. With the addition of Ni powders, a decrease in hardness was observed compared to S1 and S2. The hardness values of the coated areas are higher than the ones measured in the substrate material with an average microhardness value of 220 $HV_{0,2}$.

In Fig. 14a-c, weight losses are shown graphically under 5 N, 10 N and 15 N loads. As result, it was seen that the weight loss of the substrate was higher than the weight loss of all three coated specimens. The tribological properties of coatings depended on the type of phases, grain size, distribution of hard carbides, and elemental concentration (Erdogan et al., 2010). It is thought that the weight loss was reduced because the hardness of the carbides formed in the coated specimens was higher than the hardness value of the substrate.

Among the coated specimens, the composition coated with 70 FeCrC + 30 FeTi (% wt.) powders, which was the 2nd specimen gave the best abrasion resistance. Under a load of 15 N, the S2 specimen lost 0.4995 g of mass at the 1200 m wear distance, while the substrate AISI 1040 steel lost 6.3569 g of mass. The substrate material was worn out approximately 13 times more than the S2 specimen. The second-best result was obtained in the 1st coating made with FeCrC powder (S1). In the wear tests performed under 5 N, 10 N and 15 N loads, the weight loss of the substrate material was approximately 2 times higher than the S1 specimen. (% wt.) In the coating S3 made with the mixture of 64 FeCrC + 16 FeTi + 20 Ni powders, the weight loss was higher than S1 and S2. This was thought to be due to the reduction of carbide content in the structure. It was observed that the S3 had better abrasion resistance than the substrate material. It was determined that the weight loss of the substrate material is approximately 1.7 times higher than for the S3 specimen.

The weight losses of the specimens after the field test are shown in Fig. 15. It was noted that the weight loss of all coated specimens was lower than that of the uncoated specimen. Unlike the laboratory tests, it was observed that the least worn specimen in the field test was S3. Previous laboratory tests have established an inverse relationship between the hardness of the test samples and their wear rates. However, in the field tests, it was observed that there was a direct relationship between hardness and wear amount.

Field tests can be useful for evaluating the performance of a product or system in a more realistic setting, but they do not offer the same level of control as laboratory tests. One disadvantage of field tests is that it is often difficult to control for all of the variables that may affect the results. This can make it difficult to compare the wear performance of different test samples in a controlled way, as there may be other factors that are contributing to the wear rate.

The field tests revealed a diversity of wear patterns on the surface of the cultivator points, including scratching, ridging, chippings, and fatigue wear, caused by the impact of loose abrasive particles as shown in Fig. 16. Despite the higher hardness of the coated steel, microcutting traces were still observed, possibly owing to the alignment of the abrasive particles' sharp edges with respect to the abraded material. Comparison of samples S1 and S3, which had similar hardness, revealed that they displayed similar wear patterns and lower ploughing and chipping intensities than sample S2. Despite its higher hardness, sample S2 displayed more wear.

The variations in mass loss observed among the test specimens can be attributed to the distinct wear patterns that developed on their surfaces. Specifically, the specimen designated as "S2" (which also had the hardest coating surface) displayed higher wear in field tests compared to laboratory tests. Field tests involve more impact forces

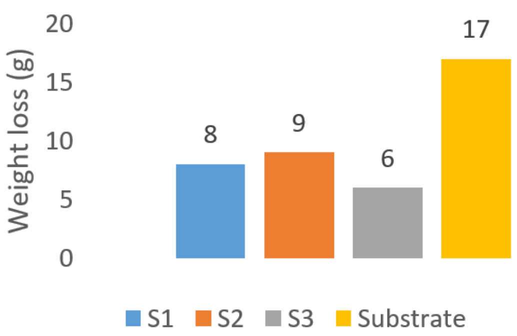

Figure 15: Weight loss of cultivator points in the field test.

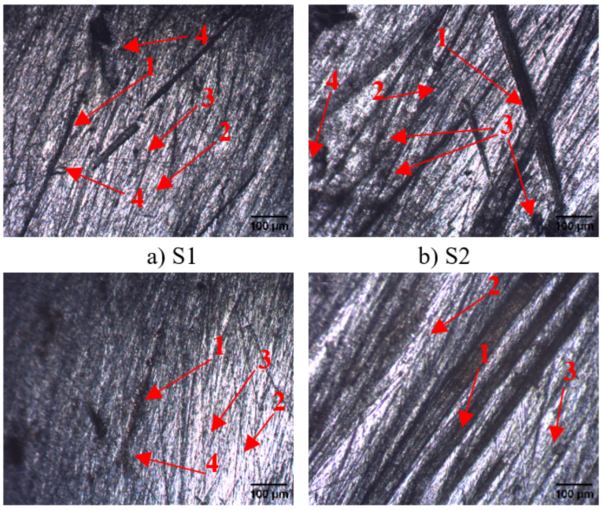

a) S1 b) S2

c) S3 d) Substrate

Figure 16: The surfaces of the tested cultivator points worn in the field test: 1-ploughing, 2-microcutting, 3-chippings, and 4-plastic deformation. Light optical microscopy.

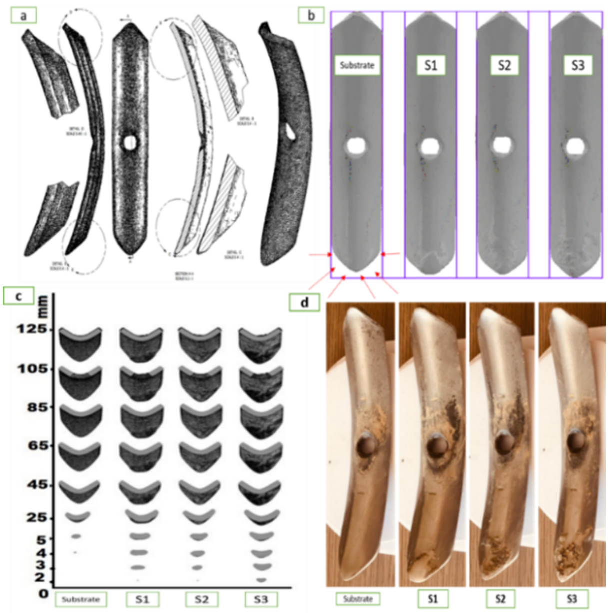

Figure 17: a) Wear in the tip of points, b) Changes in the lengths of the specimens process, c) The cross-sections obtained after the 3D scanning processes, d) Cultivator point after the field test.

compared to laboratory tests, which highlights the importance of both toughness and hardness in tillage tools, especially in field tests where impact forces are more prevalent. The results of the tests suggest that the hardness of the samples may have been a disadvantage in field tests, likely due to the presence of uncontrollable impact forces, which made the field test abrasive and damaging to the wear surface of the specimen leading to higher wear compared to laboratory tests.

In Fig. 17a, the wear in the tips of the model obtained after 3D scanning of the uncoated substrate specimen is presented. According to the detailed pictures presented in the figure, the difference between the used and unused tips after wear is seen. Changes in the lengths of the specimens are shown in Fig. 17b. The cross-sections obtained after the 3D scanning processes to determine the wear areas of the cultivator points are given in Fig. 17c. It was seen that the greatest wear occurred in the substrate, and the lowest wear occurred in the S3 specimen. In Fig. 17d, an image of the cultivator points worn as a result of the field test is given.

4. Conclusions

This study aimed to investigate the wear behavior of cultivator points made of AISI 1040 steel under field and laboratory conditions. The conclusions obtained from the study are as follows:

- It was observed that AISI 1040 steel and cultivator points produced from this steel could be successfully coated by the GTAW method using FeCrC, FeTi and Ni powders.
- No micro or macro cracks were observed in the coating layer and coating interfaces.
- The depth of the coating layer was appropriate due to the high heat input and the corresponding increase in the melting density.
- The hardness values of all coated specimens were higher than the hardness value of AISI 1040 steel.
- The maximum microhardness value (% wt.) was measured as 726.1 $HV_{0,2}$ in the specimen coated with 70 FeCrC + 30 FeTi powders. The highest average microhardness value was also measured in the same specimen as 684.73 $HV_{0,2}$.
- The highest abrasion resistance under laboratory conditions was obtained in the specimen coated with 70 FeCrC + 30 FeTi powders with the highest hardness (% wt).
- A homogeneous coating layer was formed in all specimens. While the specimens coated with (% wt.) 100 FeCrC and (% wt.) 64 FeCrC + 16 FeTi + 20 Ni powders solidified dendritic, the specimen coated with (% wt.) 70 FeCrC + 30 FeTi powders solidified to form coaxial grains with the effect of Ti element.
- It was seen that the microhardness increase in the specimens and the corresponding improvement in the wear values were caused by the formation of hard compounds such as M_7C_3, M_6C and TiC in the coating layers.
- According to the abrasion results obtained in the field tests, it was observed that the weight loss of all coated specimens was significantly less than the substrate.
- This study showed that there is a need for a new test method that includes factors such as humidity and impact to more accurately simulate field conditions. The current laboratory test used in this study does not adequately reflect real-world field tests.

5. Acknowledgments

This work was supported by the Research Fund of Tekirdag Namik Kemal University.

Project Number: NKUBAP.06.YL.18.175

References

Ardeshiri, A., Sohi, M. H., and Safaei, A. (2017). Surface alloying of A2618 aluminum with silicon and iron by TIG process. *Surf. Coatings Technol.*, 310:87–92.

Axen, N., Hogmark, S., and Jacobson, S. (2001). Friction and wear measurement techniques. In Bhushan, B., editor, *Mod. Tribol. Handb.* CRC Press, London, UK.

Bayhan, Y. (2006). Reduction of wear via hardfacing of chisel ploughshare. *Tribol. Int.*, 39(6):570–574.

Binder, M., Klocke, F., and Doebbeler, B. (2017). Abrasive wear behavior under metal cutting conditions. *Wear*, 376-377:165–171.

Blau, P. and Dehoff, R. (2013). Development of a two-body wet abrasion test method with attention to the effects of reused abradant. *Wear*, 302(1-2):1035–1039.

Burwell, J. T. (1957). Survey of possible wear mechanisms. *Wear*, 1(2):119–141.

Can, K., Dalmis, F., and Dalmis, I. (2022). Design and implementation of PLC based special purpose machine for surface coating. *Eur. J. Sci. Technol.*

Chen, Z., Zhu, Q., Wang, J., Yun, X., He, B., and Luo, J. (2018). Behaviors of 40Cr steel treated by laser quenching on impact abrasive wear. *Opt. Laser Technol.*, 103:118–125.

Cheng, J., Xu, B., Liang, X., and Wu, Y. (2008). Microstructure and mechanical characteristics of iron-based coating prepared by plasma transferred arc cladding process. *Mater. Sci. Eng. A*, 492(1-2):407–412.

Erdogan, M., Gunes, I., and Baspinar, M. S. (2010). Surface Modification of Lamellar Cast Iron with $MoSi_2$. *Electron. J. Mach. Technol.*, 7:45–54.

Eyre, T. (1976). Wear characteristics of metals. *Tribol. Int.*, 9(5):203–212.

Ghadami, F., Heydarzadeh Sohi, M., and Ghadami, S. (2015). Effect of TIG surface melting on structure and wear properties of air plasma-sprayed WC–Co coatings. *Surf. Coatings Technol.*, 261:108–113.

Gokcebay, B. (1998). *Tarım makinaları*. Ankara Üniversitesi Ziraat Fakültesi Yayınları, Ankara, Turkey.

Gulec, U. and Altuntaș, E. (2013). Determination of the material properties of the different cultivator shares. *J. Agric. Fac. Gaziosmanpaşa Univ.*, pages 13–24.

Islak, S. and Yildirim, M. (2009). The investigation of wear behaviours of SiC(p) based coatings produced by gta welding proces. *Eng. Sci.*, 4(2):227–237.

Iwaszko, J. (2006). Surface remelting treatment of plasma-sprayed Al_2O_3 + 13 wt.% TiO_2 coatings. *Surf. Coatings Technol.*, 201(6):3443–3451.

Kalácska, Á., De Baets, P., Fauconnier, D., Schramm, F., Frerichs, L., and Sukumaran, J. (2020). Abrasive wear behaviour of 27MnB5 steel used in agricultural tines. *Wear*, 442-443:203107.

Kang, A., Singh, G., and Cheema, G. (2017). Improving wear resistance via hardfacing of cultivator shovel. *Mater. Today Proc.*, 4(8):7991–7999.

Kang, A. S., Cheema, G. S., and Singla, S. (2014). Wear behavior of hardfacings on rotary tiller blades. *Procedia Eng.*, 97:1442–1451.

Kang, A. S., Grewal, J. S., Jain, D., and Kang, S. (2012). Wear behavior of thermal spray coatings on rotavator blades. *J. Therm. Spray Technol.*, 21(2):355–359.

Kostencki, P., Stawicki, T., Królicka, A., and Sędłak, P. (2019). Wear of cultivator coulters reinforced with cemented-carbide plates and hardfacing. *Wear*, 438-439:203063.

Kumar, S., Ghosh, P., and Kumar, R. (2017). Surface modification of AISI 4340 steel by multi-pass TIG arcing process. *J. Mater. Process. Technol.*, 249:394–406.

Liu, A., Guo, M., Hu, H., and Li, Z. (2008). Microstructure of Cr_3C_2-reinforced surface metal matrix composite produced by gas tungsten arc melt injection. *Scr. Mater.*, 59(2):231–234.

Malvajerdi, S. S., Malvajerdi, A. S., and Ghanaatshoar, M. (2019). Protection of CK45 carbon steel tillage tools using TiN coating deposited by an arc-PVD method. *Ceram. Int.*, 45(3):3816–3822.

Mithun, C., Sellamuthu, R., and Saravanan, R. (2018). Effect of surface modification on microstructure, hardness and wear rate of steels with 0.2%, 0.4% and 1.1 Wt%C by the addition of titanium using gas tungsten arc. *Mater. Today Proc.*, 5(2):7586–7594.

Nair, S., Sellamuthu, R., and Saravanan, R. (2018). Effect of nickel content on hardness and wear rate of surface modified cast aluminum bronze alloy. *Mater. Today Proc.*, 5(2):6617–6625.

Orhan, A. (2008). *Investigation into microstructural and wear characteristics of Fe-based coating layers produced with gas tungsten arc method*. PhD thesis, Firat University.

Polat, O., Balikoğlu, F., and Arslan, N. (2012). Experimental investigation of fatigue life of cultivators S tines. In *3. Ulus. Tasarım Imalat ve Anal. Kongresi*, Balikesir, Turkey.

Sabet, H., Khierandish, S., Mirdamadi, S., and Goodarzi, M. (2011). The microstructure and abrasive wear resistance of Fe–Cr–C hardfacing alloys with the composition of hypoeutectic, eutectic, and hypereutectic at Cr/C = 6. *Tribol. Lett.*, 44(2):237–245.

Singh, J., Chatha, S. S., and Sidhu, B. S. (2021). Abrasive wear characteristics and microstructure of Fe-based overlaid ploughshares in different field conditions. *Soil Tillage Res.*, 205:104771.

Singh, P. and Singh Chatha, S. (2020). Reduction of abrasive wear via hardfacing of mouldboard ploughshare. *Mater. Today Proc.*, 33:1505–1512.

Sundström, A., Rendón, J., and Olsson, M. (2001). Wear behaviour of some low alloyed steels under combined impact/abrasion contact conditions. *Wear*, 250(1-12):744–754.

Teker, T., Karataş, S., and Yilmaz, S. O. (2014). Microstructure and wear properties of FeCrC, FeW and feti modified Iron based alloy coating deposited by

PTA process on AISI 430 steel. *Arch. Metall. Mater.*, 59(3):925–933.

Ya-long, L., Tian-shun, D., Guo-lu, L., Hai-dou, W., Bin-Guo, F., Xiao-dong, Z., and Xiu-kai, Z. (2018). Microstructure and mechanical property of Ni-based thick coating remelted by gas tungsten arc. *Vacuum*, 155:260–269.

Yilmaz, R. (2009). Microstructure And Wear Behaviour Of Fe-Mn-C Hardfacing Alloys. In *5. Uluslararası Ileri Teknol. Sempozyumu*, Karabük, Türkiye.

Yilmaz, S. O. (2006). Wear behavior of gas tungsten arc deposited FeCr, FeCrC, and WC coatings on AISI 1018 steel. *Surf. Coatings Technol.*, 201(3-4):1568–1575.

Zabala, N., Castro, P., and Tuckart, W. (2019). Influence of roughness on the tribological behavior of a steel-steel couple lubricated with thread compound. *Lat. Am. Appl. Res.*, 49(3):193–200.

Zdravecká, E., Tkáčová, J., and Ondáč, M. (2014). Effect of microstructure factors on abrasion resistance of high-strength steels. *Res. Agric. Eng.*, 60(3):115–120.